

**Observation of excited states in the neutron-rich nucleus  $^{89}\text{Br}$** 

B. M. Nyakó<sup>1</sup>, J. Timár<sup>1,\*</sup>, M. Csatlós<sup>1</sup>, Zs. Dombrádi<sup>1</sup>, A. J. Krasznahorkay<sup>1</sup>, I. Kuti<sup>1</sup>, D. Sohler<sup>1</sup>, T. G. Tornyi<sup>1</sup>, M. Czerwiński<sup>2</sup>, T. Rząca-Urban<sup>2</sup>, W. Urban<sup>2</sup>, L. Atanasova<sup>3</sup>, D. L. Balabanski<sup>4</sup>, K. Sieja<sup>5</sup>, A. Blanc<sup>6</sup>, G. de France<sup>7</sup>, M. Jentschel<sup>6</sup>, U. Köster<sup>6</sup>, P. Mutti<sup>6</sup>, G. S. Simpson<sup>8</sup>, T. Soldner<sup>6</sup> and C. A. Ur<sup>4</sup>

<sup>1</sup>*Institute for Nuclear Research (ATOMKI), Pf. 51, 4001 Debrecen, Hungary*

<sup>2</sup>*Faculty of Physics, University of Warsaw, ul. Pasteura 5, PL-02-093 Warsaw, Poland*

<sup>3</sup>*Department of Medical Physics and Biophysics, Medical University - Sofia, 1431 Sofia, Bulgaria*

<sup>4</sup>*ELI-NP, Horia Hulubei National Institute for R&D in Physics and Nuclear Engineering IFIN-HH, 077125 Bucharest-Magurele, Romania*

<sup>5</sup>*Université de Strasbourg, IPHC, Strasbourg, France and CNRS, UMR7178, 67037 Strasbourg, France*

<sup>6</sup>*Institut Laue-Langevin, 71 avenue des Martyrs, 38042 Grenoble Cedex 9, France*

<sup>7</sup>*GANIL, CEA/DSM-CNRS/IN2P3, Bd Henri Becquerel, BP 55027, F-14076 Caen Cedex 5, France*

<sup>8</sup>*LPSC, Université Joseph Fourier Grenoble 1, CNRS/IN2P3, Institut National Polytechnique de Grenoble, F-38026 Grenoble Cedex, France*



(Received 21 June 2021; accepted 21 October 2021; published 9 November 2021)

Excited states of the neutron-rich  $^{89}\text{Br}$  have been observed for the first time. They were populated in cold-neutron induced fission of  $^{235}\text{U}$  at the PF1B facility of the Institut Laue-Langevin, Grenoble. The measurement of  $\gamma$  radiation following fission has been performed using the EXILL array of Ge detectors. The observed level structure looks similar to the yrast level structure of  $^{87}\text{Br}$ . Large valence space shell model calculations performed for  $^{89}\text{Br}$  confirmed this similarity. Comparison of the observed  $\pi g_{9/2}$  band with the results of the shell model calculations provides information on the evolution of collectivity in this region.

DOI: [10.1103/PhysRevC.104.054305](https://doi.org/10.1103/PhysRevC.104.054305)

**I. INTRODUCTION**

Exploration of single-particle energies, as well as collective behaviors of the exotic, neutron-rich nuclei near the doubly magic  $^{78}\text{Ni}$  is an important topic of contemporary nuclear-structure research. Low- and medium-spin excited states of odd-mass nuclei provide crucial information on the evolution of the single-particle energies. However, information on excited medium-spin states in this nuclear mass region is scarce. This is especially true for odd-proton neutron-rich nuclei, among which the closest isotopes northeast of  $^{78}\text{Ni}$  with known excited states are the Br isotopes. One should note that above  $N = 50$  there is only one neutron-rich nucleus among the odd-mass Br isotopes, the  $^{87}\text{Br}$ , in which medium-spin states have been explored so far [1]. Besides the information on the single-particle energies, which are important parameters in shell model calculations in this mass region, the evolution of collectivity is also expected to show differences from regions around other doubly magic nuclei. Deformed intruder configurations could appear which are predicted to be pushed down in energy due to neutron-proton correlations with enhanced quadrupole collectivity. Indeed, recent results for nuclei very close to  $^{78}\text{Ni}$  indicate a breakdown of the neutron magic number 50 and proton magic number 28 caused by a competing deformed structure [2,3]. Experimental results on low-lying levels in  $^{82,84}\text{Zn}$  [4,5] suggest that magicity is strictly confined to  $N = 50$  in  $^{80}\text{Zn}$  with

an onset of deformation developing towards heavier Zn isotopes. Further away from the  $^{78}\text{Ni}$  core, in Ge and Se isotopes,  $\gamma$  collectivity was suggested to thrive for  $N = 52$  and  $N = 54$  neutron numbers [6–8]. Sr and Zr isotopes regain sphericity close to  $N = 50$  but shape coexistence and rapid shape changes occur towards  $N = 60$ , which are possibly driven by the particle-hole excitations to the proton  $g_{9/2}$  and higher intruder orbitals, see, e.g., [9–12].

Among the Br isotopes the highest medium-spin states reflect increased collectivity in the  $N = 52$   $^{87}\text{Br}$  nucleus [1]. To investigate the evolution of collectivity in the Br isotopic chain, we aimed at studying the medium-spin states of the next even-neutron isotope, the  $N = 54$   $^{89}\text{Br}$ , which can be populated in the cold-neutron induced fission of  $^{235}\text{U}$  with reasonable yields. Using this reaction we can reach another Br isotope close to the doubly magic  $^{78}\text{Ni}$ .  $^{89}\text{Br}$  has previously been studied using the  $\beta$  decay of  $^{89}\text{Se}$  and a 130 keV transition was tentatively assigned to it [13]. However, no excited states of this nucleus have been published before our present study.

**II. EXPERIMENTAL METHODS**

The experiment was performed at the Institut Laue-Langevin (ILL) in Grenoble [14] using the PF1B cold-neutron beam. The beam was shaped into a 12 mm diameter pencil beam with a thermal equivalence flux of  $10^8/(\text{s cm}^2)$ . During two parts of the 21-d experiment  $^{235}\text{U}$  targets with  $0.525 \text{ mg/cm}^2$  and  $0.675 \text{ mg/cm}^2$  thicknesses (both enriched to 99.7%) were used. They were sandwiched, respectively,

\*Corresponding author: timar@atomki.hu

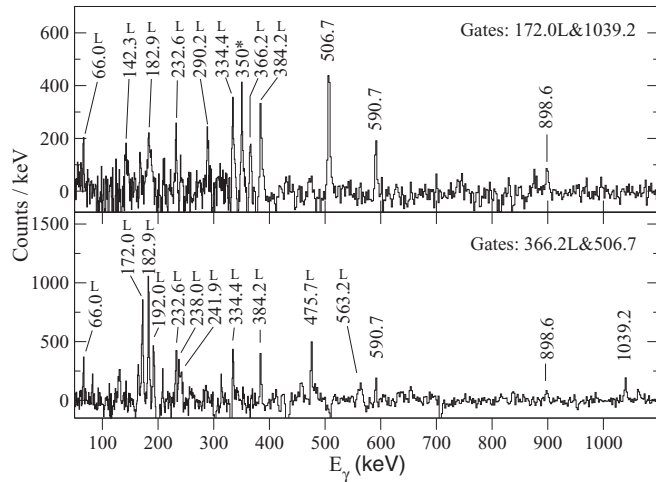


FIG. 1. Double-gated  $\gamma$ -coincidence spectra with one gate set on a strong  $^{145}\text{La}$  transition and the other gate set on one of the  $^{89}\text{Br}$  candidate transitions. Transitions labeled with L belong to  $^{145}\text{La}$ . Transition labeled with an asterisk \* belong to the contaminating  $^{106}\text{Mo}$ .

between  $15\ \mu\text{m}$  thick Zr and between  $25\ \mu\text{m}$  thick Be backings, for rapid stopping of the fission fragments. This target-backing arrangement enabled an almost Doppler-shift free measurement of the emitted  $\gamma$  rays. The  $\gamma$  rays were detected by the EXILL detector array [15] which consisted of eight Compton-suppressed EXOGAM Clover detectors [16], six Compton-suppressed GASP detectors [17] and two Clover detectors of the Lohengrin spectrometer [18]. The distance between the detectors and the target was about 15 cm. During the experiment a total of 15 terabytes of data were collected using a 100 MHz digital acquisition system in triggerless mode. In the offline analysis the triggerless events, each consisting of an energy signal and the time of its registration, were arranged into coincidence events within various time windows (from 200 to 2400 ns) and sorted into two-dimensional (2D) and three-dimensional (3D) histograms. In order to calibrate the  $\gamma$ -ray energies in the coincidence matrices, we used inner calibration lines of known transitions strongly produced in the fission process as it is described in Ref. [1]. The uncertainty of the calibration is 0.1 keV below 1200 keV  $\gamma$ -ray energy and 0.3 keV above it. The arrangement of the eight EXOGAM clover detectors of the EXILL detector array allowed the measurement of angular correlation relations of the subsequent transitions in the intense enough  $\gamma$ -decay cascades to assist in spin-parity assignments of the newly identified levels. However, the  $\gamma$  rays belonging to the  $^{89}\text{Br}$  nucleus were too weak, unfortunately, to obtain conclusive spin-parity assignments.

In order to assign  $\gamma$ -ray transitions to  $^{89}\text{Br}$  and to build the level scheme of this nucleus, 3D  $\gamma$ -ray histograms of RADWARE format [19] were created by applying a 200 ns coincidence time window. The strategy used for assigning new transitions to  $^{89}\text{Br}$  was the same as described in detail in Ref. [1]. It is based on the fact that  $\gamma$  transitions from one of the two fission fragments are in prompt coincidence with those of the other fragment. In the present case the main

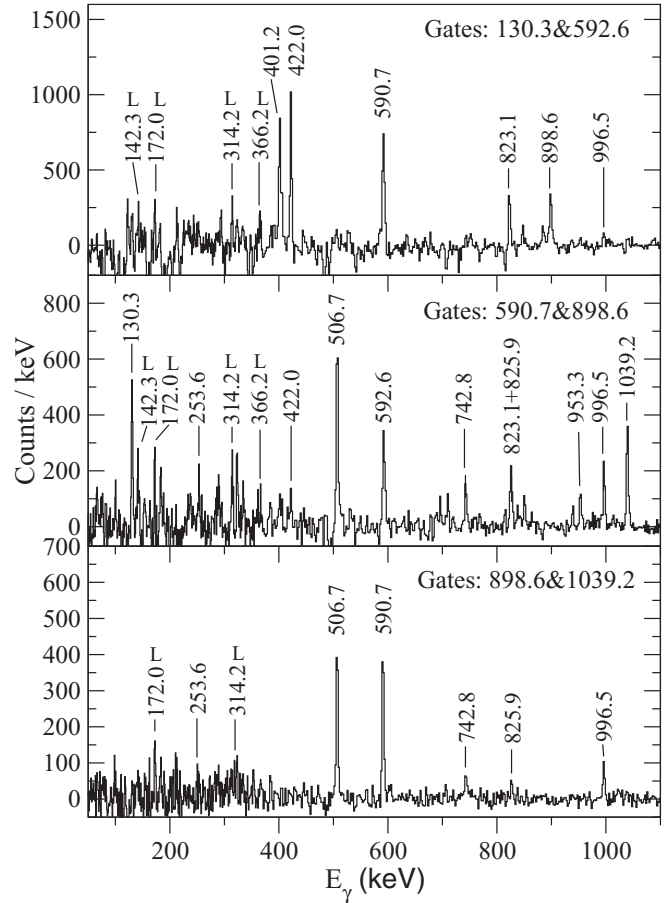


FIG. 2. Example double-gated  $\gamma$ -coincidence spectra confirming the placements of the newly observed  $^{89}\text{Br}$  transitions in the level scheme. Transitions labeled with L belong to  $^{145}\text{La}$ .

complementary fragments for  $^{89}\text{Br}$  are  $^{145}\text{La}$  and  $^{144}\text{La}$ . The level schemes of these La nuclei are rather well known from previous fission experiments [20,21]. Thus, if unknown intense  $\gamma$  rays are seen in coincidence with the strong transitions from both of these two isotopes ( $^{145}\text{La}$  and  $^{144}\text{La}$ ), they very probably belong to  $^{89}\text{Br}$ .

### III. LEVEL SCHEME

As a first step, double gates have been set on several strong transition pairs of  $^{145}\text{La}$  or of  $^{144}\text{La}$ . Besides the well-known transitions of the La isotopes, two peaks appeared in most of the double-gated spectra at 507 keV and at 1039 keV. Thus, these transitions were good candidates for decays of  $^{89}\text{Br}$  excited states. Setting double gates on one of these transitions together with a strong transition either from  $^{145}\text{La}$  or from  $^{144}\text{La}$  has provided further  $^{89}\text{Br}$ -candidate transitions, as it is seen in the example spectra plotted in Fig. 1. To analyze the coincidence relations between these newly observed transitions, double gates have been set on them. Besides the derivation of their coincidence relations, other new transitions have also been found, as it is shown in Fig. 2. They are in coincidence with the strong transitions of  $^{145}\text{La}$ , but they do not belong to any known level schemes. Therefore, they

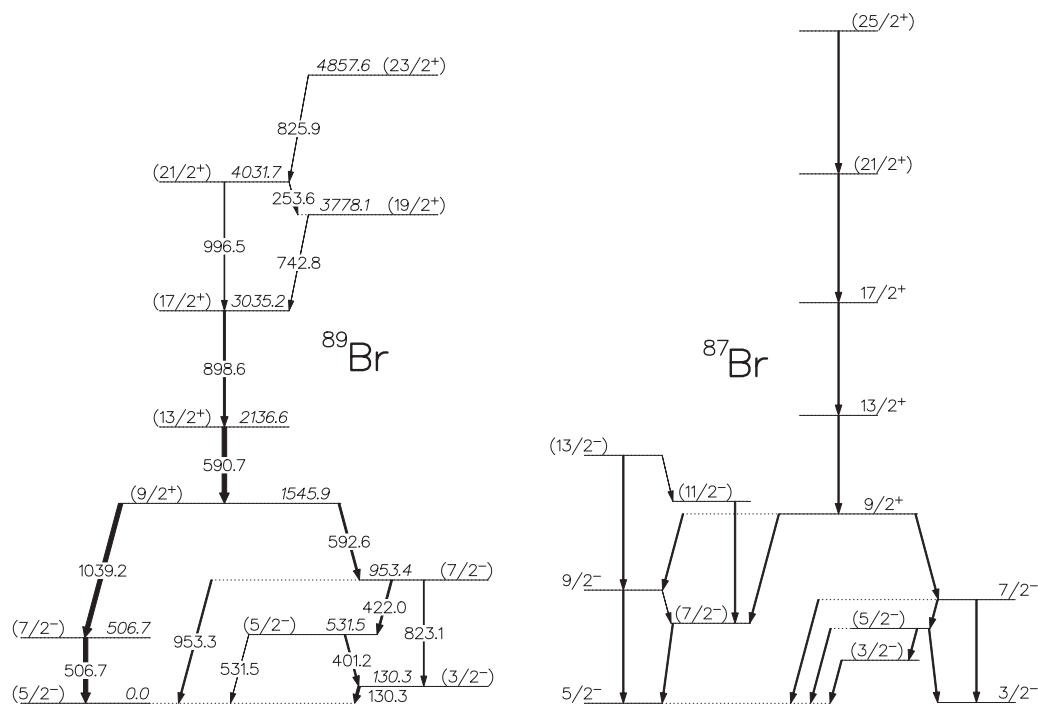


FIG. 3. (Left) Experimental level scheme of  $^{89}\text{Br}$  obtained in the present work. The  $\gamma$ -ray and level energies (in italics) are given in keV, the width of the transitions are proportional with their relative intensities. (Right) Skeleton medium-spin level scheme of  $^{87}\text{Br}$  taken from Ref. [1].

should belong to  $^{89}\text{Br}$ . Based on their coincidence relations the level scheme of  $^{89}\text{Br}$  has been built, which is plotted in the left side of Fig. 3.

The derived level energies, the energies and relative intensities of the  $\gamma$  rays, as well as their placement in the level scheme are presented in Table I.

TABLE I. Level energies, spin-parities,  $\gamma$ -ray energies, and relative intensities, as well as  $\gamma$ -ray branching ratios corresponding to the observed level scheme of  $^{89}\text{Br}$ . The relative intensities are normalized to that of the strong 1039.2 keV transition.

| $E_i$     | $I_i^\pi$            | $E_f$  | $E_\gamma$ | $I_\gamma$ | BR      |
|-----------|----------------------|--------|------------|------------|---------|
| 0.0       | (5/2 <sup>-</sup> )  |        |            |            |         |
| 130.3(3)  | (3/2 <sup>-</sup> )  | 0.0    | 130.3(3)   | >46        |         |
| 506.7(3)  | (7/2 <sup>-</sup> )  | 0.0    | 506.7(3)   | >100       |         |
| 531.5(3)  | (5/2 <sup>-</sup> )  | 0.0    | 531.5(3)   | >9         | 29(13)  |
|           |                      | 130.3  | 401.2(3)   | >31        | 100(29) |
| 953.4(3)  | (7/2 <sup>-</sup> )  | 0.0    | 953.3(5)   | 31(6)      |         |
|           |                      | 130.3  | 823.1(4)   | 14(6)      |         |
|           |                      | 531.5  | 422.0(3)   | 40(6)      |         |
| 1545.9(4) | (9/2 <sup>+</sup> )  | 506.7  | 1039.2(4)  | 100(9)     |         |
|           |                      | 953.4  | 592.6(8)   | 40(9)      |         |
| 2136.6(5) | (13/2 <sup>+</sup> ) | 1545.9 | 590.7(3)   | 100(9)     |         |
| 3035.2(7) | (17/2 <sup>+</sup> ) | 2136.6 | 898.6(4)   | 43(4)      |         |
| 3778.1(7) | (19/2 <sup>+</sup> ) | 3035.2 | 742.8(4)   | 8(2)       |         |
| 4031.7(7) | (21/2 <sup>+</sup> ) | 3035.2 | 996.5(4)   | 13(3)      |         |
|           |                      | 3778.1 | 253.6(6)   | 2(1)       |         |
| 4857.6(9) | (23/2 <sup>+</sup> ) | 4031.7 | 825.9(5)   | 9(3)       |         |

The observation of the 130.3 keV  $\gamma$  ray, which is identified as the transition from the first excited state to the ground state, is supporting the tentative assignment of this transition to  $^{89}\text{Br}$  by Ref. [13].

The relative intensities of the  $\gamma$  transitions were derived from double-gated  $\gamma$ -ray spectra. To determine the intensity of a particular transition in a  $\gamma$  cascade a double gate has to be set below that transition. Thus, the intensity of a transition can only be determined this way, if at least two transitions exist below it. For this reason, only lower limits could be given for the relative intensities of the transitions depopulating the first three excited states of  $^{89}\text{Br}$ . These limits are based on the total intensities feeding the actual levels, and on the branching ratios of their depopulating transitions. The branching ratios for a level can be determined by setting double gates above that level, based on which, it was possible to derive the branching ratios for the third excited level (see Table I).

The obtained level scheme is very similar to the medium-spin level scheme of  $^{87}\text{Br}$ . In order to show the similarity between the two level schemes, the “skeleton” medium-spin level scheme of  $^{87}\text{Br}$  is also plotted in the right side of Fig. 3. Although spins and parities for the new levels could not be derived from angular correlation relations of the subsequent transitions, the similarity between the two level schemes allowed the assignment of tentative spin-parities to the levels in the new level scheme to be made. These tentative spin-parities are also presented in Table I. A clear difference between the high-spin parts of the two level schemes is that in  $^{89}\text{Br}$  the (19/2<sup>+</sup>) and (23/2<sup>+</sup>) levels were observed, while in  $^{87}\text{Br}$  they were not observed. These states may belong to the signature-partner band. In this case their appearance

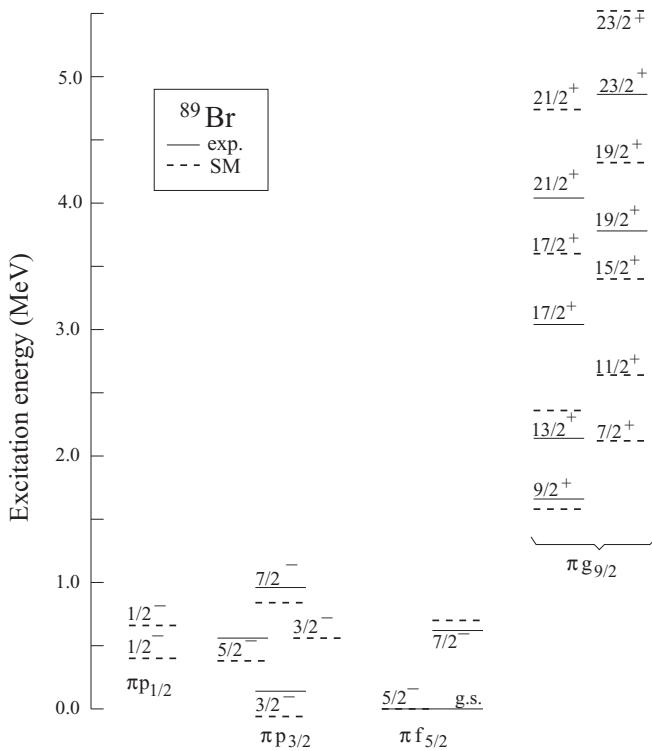


FIG. 4. Comparison of the observed (exp.) and calculated (SM) levels of  $^{89}\text{Br}$ .

indicates that the signature splitting in  $^{89}\text{Br}$  is smaller than it is in  $^{87}\text{Br}$ .

#### IV. DISCUSSION

We compared the obtained level scheme with the results of the contemporary shell-model calculations using a large valence space outside the  $^{78}\text{Ni}$  core, including the  $1f_{5/2}$ ,  $2p_{3/2}$ ,  $2p_{1/2}$ ,  $1g_{9/2}$  orbitals for protons and the  $2d_{5/2}$ ,  $3s_{1/2}$ ,  $1g_{7/2}$ ,  $1d_{3/2}$ ,  $1h_{11/2}$  orbitals for neutrons. The model and the parameters of the calculations are the same as used in Refs. [1,22] for  $^{87}\text{Br}$  and in many other studies of nuclei in this region, e.g., in Refs. [23–28]. The full-space diagonalization of the Hamiltonian was achieved using the shell-model code ANTOINE [29,30].

The experimental and calculated level energies, spin-parities, and dominating configurations are plotted in Fig. 4. The tentative experimental spin-parities are rather well reproduced by the calculations. The level energies are also reasonably well reproduced for the states belonging to the low-spin structure built on the  $(5/2^-)$  ground state and to the low-spin structure built on the  $(3/2^-)$  first excited state. According to the calculations, these structures belong to the  $\pi f_{5/2}$  and  $\pi p_{3/2}$  configurations, respectively. They show, however, a large fragmentation of all the calculated wave functions. The dominant components  $\nu d_{5/2}^4 \pi f_{5/2}^2 p_{3/2}^3$  for the  $\pi p_{3/2}$  band and  $\nu d_{5/2}^4 \pi f_{5/2}^3 p_{3/2}^2$  for the  $\pi f_{5/2}$  band do not exceed 30%. All other configurations count a few percent each. Both  $1/2^-$  states predicted by the model are due to the occupation of the  $p_{1/2}$  orbital, by 1.0 and 0.75 particle, respec-

tively. As in the cases of two other negative-parity structures, the dominating component  $\nu d_{5/2}^4 \pi f_{5/2}^2 p_{3/2}^3 p_{1/2}^1$  counts for only 28% and 10%, respectively, and all other configurations are of even smaller fractions. The large fragmentation of the wave functions, typical for collective nuclei, appears common in many shell-model studies in this region. In particular, a substantial mixing between protons in the  $p_{3/2}$  and the  $f_{5/2}$  orbitals is favoured due to the small single-particle splitting in the  $^{78}\text{Ni}$  core.

The present calculation reproduces accurately also the position of the  $9/2^+$  state and suggests it to come from the  $\pi g_{9/2}^1$  orbital population, with 40% of  $\pi g_{9/2}^1 \otimes \nu 0^+$  configuration. The  $13/2^+$  level, predicted by the model as a coupling of the odd proton in  $g_{9/2}$  to the neutron  $2^+$ , is matching the experimental counterpart within 260 keV. Starting from the  $17/2^+$  state, the disagreement between the model and experiment becomes substantial. The upper part of the spectrum is calculated more than 600 keV too high, though the energy differences relative to the  $17/2^+$  level are still well reproduced. The  $9/2^+ - 17/2^+$  states have one proton in the  $g_{9/2}$  orbital with neutrons occupying predominantly the  $d_{5/2}$  and  $s_{1/2}$  orbits. This changes in the  $21/2^+$  state where one neutron is promoted to the  $g_{7/2}$  orbital. The  $19/2^+$  and  $23/2^+$  levels involve one neutron in the  $h_{11/2}$  orbit.

To have a better understanding on the observed discrepancies, the proton-neutron couplings of the concerned states were examined. The composition of the  $17/2^+$  state reveals 31% of the  $\pi g_{9/2}^1 \otimes \nu 4^+$  component and 37% of the protons forming a  $13/2^+$  state coupled to  $\nu 2^+$ . The position of the  $2^+$  state in  $^{88}\text{Se}$ , ascribed predominantly to the neutron configuration, was accurately reproduced by the present shell-model calculation [6]. However, larger deviations were found for the  $4^+$  and higher excited states. Also, employing high effective charges in this region appeared necessary to obtain correct values of the  $E2$  reduced transition probabilities [7,12]. This was understood as due to the missing contributions from the orbits outside the model space which are necessary for the development of quadrupole collectivity. In  $^{87}\text{Br}$  a similar discrepancy for the  $g_{9/2}$  band was noted as in  $^{89}\text{Br}$ , thus we conclude on enhanced collectivity of these bands in both bromine isotopes. On the other hand, the results of the calculations confirm that the signature splitting in  $^{89}\text{Br}$  is smaller than it is in  $^{87}\text{Br}$ , which seems to be in agreement with the experimental observations.

#### V. SUMMARY

In summary, excited states of the neutron-rich  $^{89}\text{Br}$  nucleus have been observed experimentally for the first time. They were studied by means of in-beam  $\gamma$  spectroscopy of  $^{235}\text{U}(n, f)$  fission fragments, using the EXILL Ge detector array. The fission has been induced by the cold-neutron beam of the PF1B facility of the Institut Laue-Langevin, Grenoble. The observed level scheme has been found to be very similar to the medium-spin level scheme of  $^{87}\text{Br}$ . This similarity enabled us to assign tentative spin-parities to the newly observed levels. The experimental level scheme was compared to the results of contemporary shell model calculations. The energies of the lower-energy levels and their spin-parities are

well reproduced by the calculations. It has been found that the main configuration components of the observed three band-like structures are  $\pi f_{5/2}$ ,  $\pi p_{3/2}$ , and  $\pi g_{9/2}$ , although the wave functions are rather fragmented, which is typical for collective nuclei. Similarly to the case of  $^{87}\text{Br}$ , the highest levels of the  $\pi g_{9/2}$  band could not be well described, probably due to the missing contributions from the orbits outside the model space which are necessary for the development of quadrupole collectivity. Thus we conclude on enhanced collectivity of these bands in both bromine isotopes. On the other hand, the calculations reproduce that the observed signature splitting in  $^{89}\text{Br}$  is smaller than in  $^{87}\text{Br}$ .

#### ACKNOWLEDGMENTS

The authors thank the technical services of the ILL, LPSC, and GANIL for supporting the EXILL campaign.

The EXOGAM Collaboration and the INFN Legnaro are acknowledged for the loan of Ge detectors. This work was supported by the National Research, Development and Innovation Fund of Hungary, financed under the K18 funding scheme with Project nos. K128947 and K124810, as well as by the European Regional Development Fund (Contract No. GINOP-2.3.3-15-2016-00034). This work was also supported by the Polish National Science Centre under Contract No. DEC-2013/09/B/ST2/03485 and by the Bulgarian National Science Fund Contract No. KP-06-N48/1. I.K. was supported by National Research, Development and Innovation Office - NKFIH, Contract No. PD 124717. D.L.B. acknowledges support from the Extreme Light Infrastructure Nuclear Physics (ELI-NP) Phase II, a project co-financed by the Romanian Government and the European Union through the European Regional Development Fund, the Competitiveness Operational Programme (1/07.07.2016, COP, ID 1334).

- 
- [1] B. M. Nyakó, J. Timár, M. Csatlós, Zs. Dombrádi, A. Krasznahorkay, I. Kuti *et al.*, *Phys. Rev. C* **103**, 034304 (2021).
- [2] F. Nowacki, A. Poves, E. Caurier, and B. Bounthong, *Phys. Rev. Lett.* **117**, 272501 (2016).
- [3] R. Taniuchi *et al.*, *Nature (London)* **569**, 53 (2019).
- [4] Y. Shiga, K. Yoneda, D. Steppenbeck, N. Aoi, P. Doornenbal, J. Lee, H. Liu, M. Matsushita, S. Takeuchi, H. Wang, H. Baba, P. Bednarczyk, Z. Dombradi, Z. Fulop, S. Go, T. Hashimoto, M. Honma, E. Ideguchi, K. Ieki, K. Kobayashi, Y. Kondo, R. Minakata, T. Motobayashi, D. Nishimura, T. Otsuka, H. Otsu, H. Sakurai, N. Shimizu, D. Sohler, Y. Sun, A. Tamii, R. Tanaka, Z. Tian, Y. Tsunoda, Z. Vajta, T. Yamamoto, X. Yang, Z. Yang, Y. Ye, R. Yokoyama, and J. Zenihiro, *Phys. Rev. C* **93**, 049904(E) (2016).
- [5] C. M. Shand *et al.*, *Phys. Lett. B* **773**, 492 (2017).
- [6] I. N. Gratchev, G. S. Simpson, G. Thiamova, M. Ramdhane, K. Sieja, A. Blanc, M. Jentschel, U. Köster, P. Mutti, T. Soldner, G. de France, C. A. Ur, and W. Urban, *Phys. Rev. C* **95**, 051302(R) (2017).
- [7] K. Sieja, T. R. Rodríguez, K. Kolos, and D. Verney, *Phys. Rev. C* **88**, 034327 (2013).
- [8] M. Lettmann *et al.*, *Phys. Rev. C* **96**, 011301(R) (2017).
- [9] T. Togashi, Y. Tsunoda, T. Otsuka, and N. Shimizu, *Phys. Rev. Lett.* **117**, 172502 (2016).
- [10] J.-M. Régis, J. Jolie, N. Saed-Samii, N. Warr, M. Pfeiffer, A. Blanc, M. Jentschel, U. Köster, P. Mutti, T. Soldner, G. S. Simpson, F. Drouet, A. Vancraeynest, G. de France, E. Clement, O. Stezowski, C. A. Ur, W. Urban, P. H. Regan, Z. Podolyak, C. Larijani, C. Townsley, R. Carroll, E. Wilson, L. M. Fraile, H. Mach, V. Pazy, B. Olaizola, V. Vedia, A. M. Bruce, O. J. Roberts, J. F. Smith, M. Scheck, T. Kroll, A. L. Hartig, A. Ignatov, S. Ilieva, S. Lalkovski, W. Korten, N. Marginean, T. Otsuka, N. Shimizu, T. Togashi, and Y. Tsunoda, *Phys. Rev. C* **95**, 054319 (2017).
- [11] E. Clement *et al.*, *Phys. Rev. Lett.* **116**, 022701 (2016).
- [12] K. Sieja, F. Nowacki, K. Langanke, and G. Martinez-Pinedo, *Phys. Rev. C* **79**, 064310 (2009).
- [13] K. Rengan, J. Lin, M. Zendel, and R. A. Meyer, *Nucl. Instrum. Methods* **197**, 427 (1982).
- [14] H. Abele *et al.*, *Nucl. Instrum. Methods Phys. Res. A* **562**, 407 (2006).
- [15] M. Jentschel *et al.*, *JINST* **12**, P11003 (2017).
- [16] J. Simpson *et al.*, *Acta Phys. Hung. New Ser.: Heavy Ion Phys.* **11**, 159 (2000).
- [17] D. Bazzacco *et al.*, in *Proceedings of the 5th International Seminar on Nuclear Physics*, edited by A. Covello (World Scientific, Singapore, 1999), p. 417430.
- [18] G. S. Simpson, J. C. Angélique, J. Genevey, J. A. Pinston, A. Covello, A. Gargano, U. Köster, R. Orlandi, and A. Scherillo, *Phys. Rev. C* **76**, 041303(R) (2007).
- [19] D. C. Radford, *Nucl. Instrum. Methods Phys. Res. A* **361**, 297 (1995).
- [20] W. Urban, W. R. Phillips, J. L. Durell, M. A. Jones, M. Leddy, C. J. Pearson, A. G. Smith, B. J. Varley, I. Ahmad, L. R. Morss, M. Bentalab, E. Lubkiewicz, and N. Schulz, *Phys. Rev. C* **54**, 945 (1996).
- [21] Y. X. Luo *et al.*, *Nucl. Phys. A* **818**, 121 (2009).
- [22] J. Wiśniewski, W. Urban, M. Czerwiński, J. Kurpeta, A. Płochocki, M. Pomorski, T. Rząca-Urban, K. Sieja, L. Canete, T. Eronen, S. Geldhof, A. Jokinen, A. Kankainen, I. D. Moore, D. A. Nesterenko, H. Penttilä, I. Pohjalainen, S. Rinta-Antila, A. de Roubin, and M. Vilén, *Phys. Rev. C* **100**, 054331 (2019).
- [23] M. Czerwiński, T. Rząca-Urban, K. Sieja, H. Sliwiska, W. Urban, A. G. Smith, J. F. Smith, G. S. Simpson, I. Ahmad, J. P. Greene, and T. Materna, *Phys. Rev. C* **88**, 044314 (2013).
- [24] T. Materna, W. Urban, K. Sieja, U. Köster, H. Faust, M. Czerwiński, T. Rząca-Urban, C. Bernards, C. Fransen, J. Jolie, J.-M. Régis, T. Thomas, and N. Warr, *Phys. Rev. C* **92**, 034305 (2015).
- [25] M. Czerwiński, T. Rząca-Urban, W. Urban, P. Bączyk, K. Sieja, B. M. Nyakó, J. Timár, I. Kuti, T. G. Tornyi, L. Atanasova, A. Blanc, M. Jentschel, P. Mutti, U. Köster, T. Soldner, G. de France, G. S. Simpson, and C. A. Ur, *Phys. Rev. C* **92**, 014328 (2015).
- [26] M. Czerwiński, T. Rząca-Urban, W. Urban, P. Bączyk, K. Sieja, J. Timár, B. M. Nyakó, I. Kuti, T. G. Tornyi, L. Atanasova *et al.*, *Phys. Rev. C* **93**, 034318 (2016).

- [27] M. Czerwiński, K. Sieja, T. Rząca-Urban, W. Urban, A. Płochocki, J. Kurpeta, J. Wiśniewski, H. Penttilä, A. Jokinen, S. Rinta-Antila, L. Canete, T. Eronen, J. Hakala, A. Kankainen, V. S. Kolhinen, J. Koponen, I. D. Moore, I. Pohjalainen, J. Reinikainen, V. Simutkin, A. Voss, I. Murray, and C. Nobs, *Phys. Rev. C* **95**, 024321 (2017).
- [28] T. Rząca-Urban, M. Czerwiński, W. Urban, A. G. Smith, I. Ahmad, F. Nowacki, and K. Sieja, *Phys. Rev. C* **88**, 034302 (2013).
- [29] E. Caurier and F. Nowacki, *Acta Phys. Pol. B* **30**, 705 (1999).
- [30] E. Caurier, G. Martínez-Pinedo, F. Nowacki, A. Poves, and A. P. Zuker, *Rev. Mod. Phys.* **77**, 427 (2005).